Forthcoming in *Review of Philosophy and Psychology*

On the retinal origins of the Hering primaries[1]

Wayne Wright

Abstract: This paper argues that the distinctiveness of the Hering primary hues – red, green, blue, and yellow – is already evident at the retina. Basic features of spectral sensitivity provide a foundation for the development of unique hue perceptions and the hue categories of which they are focal examples. Of particular importance are locations in color space at which points of minimal and maximal spectral sensitivity and extreme ratios of chromatic to achromatic response occur. This account builds on Jameson & D'Andrade's (1997) insight about the relationship between the Hering primaries and chromatic/achromatic ratios, Romney & Chiao's (2009) color appearance model, and Thornton's (1971; 1999) research on artificial lighting.

1. Introduction

Hue is the most psychologically significant aspect of color appearance. Hues are denominated by terms such as 'red', 'blue', 'green', and 'yellow', and color naming tends to be based on hue, at least in Western industrialized societies. The four hues just listed, the "Hering primaries," are thought to have a privileged status amongst the hues. Particularly influential is the idea that every perceived hue can be fully described in terms of amounts of the Hering primaries seen "in" it. According to the experimental literature on hue scaling, unique hues are judged to consist 100% of a single primary and binary hues are judged to contain amounts of two primaries, with some pairings being impossible; e.g., one orange might be 60% yellow and 40% red while another has balanced yellow and red components, but no hue is seen as parts both red and green. Relatedly, it

[1] I would like to thank Kimberly Jameson, A. Kimball Romney, Michael Webster, and Jeff Yoshimi for comments on drafts of this paper and discussions about the issues addressed herein. A special debt of thanks is owed to Justin Broackes and an anonymous referee of this journal, as their feedback was of immense help to my thinking about these matters.

is hard to fathom how a given greenish hue might look to have certain amounts of teal and chartreuse in it (Abramov & Gordon 1994, p.468). On the picture that emerges, (i) the hues occupy a two-dimensional space with red/green and yellow/blue cardinal, orthogonal axes, (ii) chromatic stimuli falling on one of those axes have a unique hue, and (iii) all chromatic stimuli not on a cardinal hue axis have a binary hue that is a blend of the two elementary hues defining the quadrant in which they are located. It has been further supposed that (iv) these three features are due to the opponent processing architecture of the human visual system; see Byrne & Hilbert (2003, pp.14-15), De Valois & Jacobs (1968, p.538), and Tye (2000, pp.159-161).

Claim (iv), although still influential, is beset by empirical difficulties; see Abramov & Gordon (1994; 2005), Jameson & D'Andrade (1997), and MacLeod (2010). Other attempts to tie the Hering primaries to neural processing have not fared any better. Rolf Kuehni (2005, p.402) has remarked that "[it] remains to be seen if Hering's [unique hues] have specific neurophysiological correlates or if [unique hues] are … accidental psychological reference points." As for (i)-(iii), Jameson & D'Andrade (1997) are among the few to recently dissent from them. They agree that the Hering primaries have a "special salience," but contend that it stems from irregularities in perceptual color space, not from all hues being organized around axes defined by the Hering primaries. While I am sympathetic to much of Jameson & D'Andrade's alternative perspective, my concern now is only to use certain of their ideas to address the issue of neural basis. Most important is Jameson & D'Andrade's (p.314) undeveloped suggestion that the Hering primaries are perceptually conspicuous because they coincide in color space with locations having significant achromatic and chromatic sensitivity properties. The account given here is consistent with Jameson & D'Andrade's broader framework, but it could also be adopted into a view more amenable to (i)-(iii).

The paper focuses on sensitivity at the front end of the visual system, building on, in addition to Jameson & D'Andrade's work, Romney & Chiao's (2009) color appearance model based on the sensitivities of retinal cone photoreceptor cells and William Thornton's (1971; 1999) research on spectral sensitivity and artificial lighting. The first two sections that follow discuss key details from both sources in setting the stage for the paper's novel contributions. The paper's central claim is that the distinctiveness of the Hering primaries is to considerable extent already evident at the retina, due to how features of spectral sensitivity figure in color space.

Before embarking, clarification of the current effort's ambitions is in order. It is not being claimed that the particular phenomenologies of the Hering primaries are determined by low-level visual processes, nor that all structural relations amongst the hues can be explained by such processes. Additionally, no attempt is made to specify unique hue choices for individual observers. Rather, the goal is to demonstrate that as early as the retina, certain locations in color space are marked out in a way that provides a footing for the development of unique hue perceptions and the hue categories of which they are focal examples. The proposed account can be only part of the entire story about the Hering primaries, as is evident from the widespread variability across normal subjects in the selection of stimuli exemplifying the unique hues. Individual subjects' unique hue choices cannot be reliably predicted by any extant model of color vision. Higher-level visual mechanisms, as well as cognitive, environmental and cultural factors, surely contribute to inter alia which stimuli are selected as unique blue by a given perceiver. The account offered here, however, ought to enable progress in studying those contributions, as it reveals a baseline condition for the emergence of hue categories and focal examples of them at the periphery of the visual system.

2. Romney& Chiao's color appearance model

Romney & Chiao (2009) present a model, assembled from different ideas already in the color literature, for calculating the appearance of Munsell color chips based on their reflectance spectra and the sensitivity curves of human cone cells; the Munsell Hue circle is shown in figure 1.[2] Their model addresses a simple situation: one chip viewed against a neutral background under an illuminant with a flat power spectrum, independent of post-receptoral adaptation. The specific calculations of their model have no known neurophysiological analogs, but Romney & Chiao believe the visual system performs operations that issue similar results (p.10376). They also note that a five-layer neural network can perform operations equivalent to those in their model (p.10380). Their model places the Munsell chips in a space that is tightly correlated with CIE L*a*b* space. While Romney & Chiao use their model to address several questions about color

[2] The Munsell color system is based on the concepts of Hue, Value, and Chroma. These attributes provide for a three-dimensional, sphere-like color solid:

- Value (lightness) is the vertical dimension. Steps along the axis run from 0 (black) to 10 (white).
- Radii from the achromatic axis define different Hues. Hues are organized into ten equally spaced sectors determined by five principal Hues (the Hering primaries plus purple) and five intermediate pairings of them, with numbered gradations within each hue category. Each Hue sector has 10 steps and it is common to display the Hue circle using 2.5 step intervals, as in figure 1.
- Steps along each radial spoke indicate Chroma (roughly, saturation, level of purity). Stimuli with Chroma zero are achromatic and different combinations of Hue and Value have their own maximum Chroma.

The standard format for referring to locations in Munsell space is Hue Value/Chroma. For example, chip 2.5RP 6/4 has step 2.5 of Hue RP (Red-Purple), Value 6, and Chroma 4.

vision, their presentation of it does not take up hue categories or unique hues. Here, I summarize and replicate Romney & Chiao's model so as to utilize it in tackling those phenomena.[3]

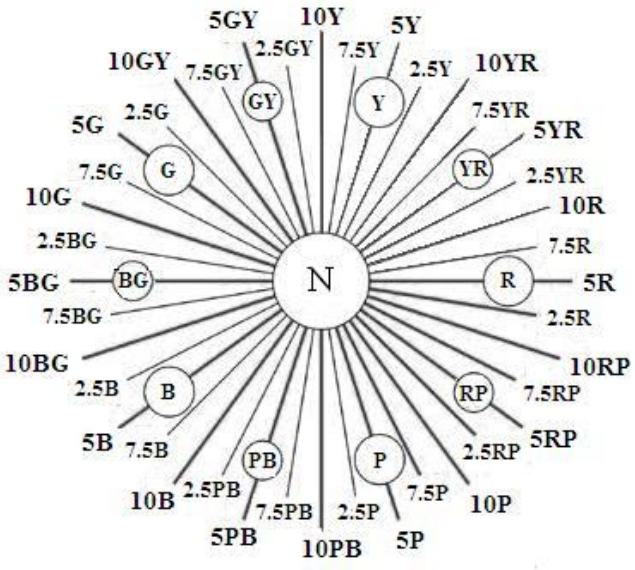

Figure 1: The Munsell Hue circle. R: Red; YR: Yellow-Red; Y: Yellow; GY: Green-Yellow; G: Green; BG: Blue-Green; B: Blue; PB: Purple-Blue; P: Purple; RP: Red-Purple; N: Neutral. Steps 2.5, 5, 7.5, and 10 shown for each hue.

Romney & Chiao use reflectance spectra from 400-700 nm of 1269 painted Munsell chips and Stockman & Sharpe's (2000) sensitivity curves for human cone cells. The present analysis employs the same cone curves,[4] with reflectance spectra at 5 nm intervals in the visible band for the following 727 objects:

[3] The following calculations were done using Microsoft Excel and OpenOffice Calc. Singular value decomposition was performed with PopTools for Excel (http://www.cse.csiro.au/poptools/).

[4] The cone sensitivity curves are on-line at http://www-cvrl.ucsd.edu/cones.htm.

From the University of Joensuu Color Group[5]

- Four hundred fifty five Munsell chromatic chips at four Hue steps (2.5, 5, 7.5, 10) from the standard ten sectors, at medium Value levels (4, 5, 6), and weak-to-middle Chroma levels (2, 4, 6, 8). A full set of Chroma samples is not available for some combinations of Hue and Value.
- Six Munsell achromatic chips (N3-8).
- One hundred seventy seven plant surfaces with generic color labels assigned by the researchers who measured them.

From the United States Geological Survey Digital Spectral Library[6]

- Twenty arbitrarily selected minerals (e.g., cinnabar, endelite, nephrite).
- Five familiar man-made surfaces (e.g., red brick, yellow terrycloth).

From the Bee Sensory and Behavioural Ecology Lab[7]

- Sixty plant surfaces, consisting of the first fifteen entries, organized by increasing database ID number, returned from searches for samples that are categorized in the database as appearing red, green, blue, or yellow to human observers.

From Changizi et al (2006)

- African American, Asian, Caucasian (light), and East Asian (dark) human skin.

[5] These data are on-line at http://spectral.joensuu.fi/index.php?page=database. The original spectrophotometer-measured Munsell spectra are used. The plant samples were measured with acoutso-optic tunable filters (AOTF). Since AOTF-measured Munsell spectra must be multiplied by ca. 0.8 in order to produce curves that agree with spectrophotometer-measured spectra, I multiplied these plant reflectances by 0.8. Some samples were discarded due to gross underestimation of short wavelength reflectance by AOTF (Kohonen et al 2006, p.383).

[6] These data are on-line at http://speclab.cr.usgs.gov/spectral.lib06/ds231/datatable.html.

[7] These spectra are on-line at http://reflectance.co.uk/new/index.php.

The use of only ca. 35% of the Munsell samples analyzed by Romney & Chiao and the inclusion of many samples that they did not, was prompted by an interest in naturalistic stimuli; one might entertain some worry that the features of achromatic and chromatic sensitivity emphasized later are mere artifacts, were high Value and high Chroma stimuli included. The Value and Chroma ranges of the Munsell chips used here are within the bounds of those found in many natural environments and the additional natural and man-made samples increase the breadth of the data set. The plant samples are also relevant to the application of Romney & Chiao's model to this paper's concerns.

Romney & Chiao begin by reducing redundancy in the overlapping cone sensitivities through singular value decomposition (SVD). SVD factorizes an n x m matrix R ($n \geq m$) into $R = UDV^T$, where U is an n x m "hanger" matrix, D is a diagonal m x m "stretcher" matrix consisting of the singular values, and V is an m x m "aligner" matrix. In this case, there is sensitivity at n wavelength intervals in m cone classes. Importantly, the resulting hanger matrix is an orthogonalization of the cone sensitivities. Buchsbaum & Gottschalk (1983) demonstrate that orthogonalized cone sensitivities yield optimal coding for efficient information transmission. Such efficiency is crucial, as only about one million fibers leave each eye through the optic nerve, while each retinal mosaic contains around 120 million photoreceptor cells (ca. six million of which are cones). An assumption of the model is that optimally efficient transmission is approximated by the retina.

There are infinitely many orthogonalizations of the cone curves, all related to one another by linear transformations of the cone sensitivities by 3 x 3 matrices (MacAdam 1953); e.g., Kries/Ives gain control transformations of cone outputs. Romney & Chiao exploit previous work by Jozef Cohen and his colleagues to address this complication; see Burns et al (1990) and

Cohen (2001). They construct a projection matrix, P, by post-multiplying any U matrix obtained through an SVD of transformed cone sensitivity curves by its transpose; see also Koenderink & van Doorn (2003). This operation "washes away" the contribution of the linear transformation, yielding a matrix that is invariant across all linear transformations of the cone sensitivities.

Romney & Chiao's approach thus far follows that of Cohen and his collaborators. Romney & Chiao's next step, to cube-root (element-wise) the reflectance spectra before post-multiplying them by the projection matrix, is novel. The cube-rooted reflectance spectra are run through the projection matrix, generating a matrix S. Their final step is to scale the reflectance spectra in a three-dimensional space by taking an SVD on S. Each spectrum's location in the space is given by a row vector in the scaling SVD's hanger matrix. The dimensions of that space are linear transforms of the cone sensitivity curves and provide a "spectral envelope" representing the sensitivity of the human eye to different wavelengths of light throughout the 400-700 nm range in each of three components (Romney & Chiao, p.10379). Figure 2 displays the three components derived from the present analysis, which are column vectors of the aligner matrix of the scaling SVD; these match (aside from arbitrary change of sign) those of Romney & Chiao (p.10380, fig.3D).

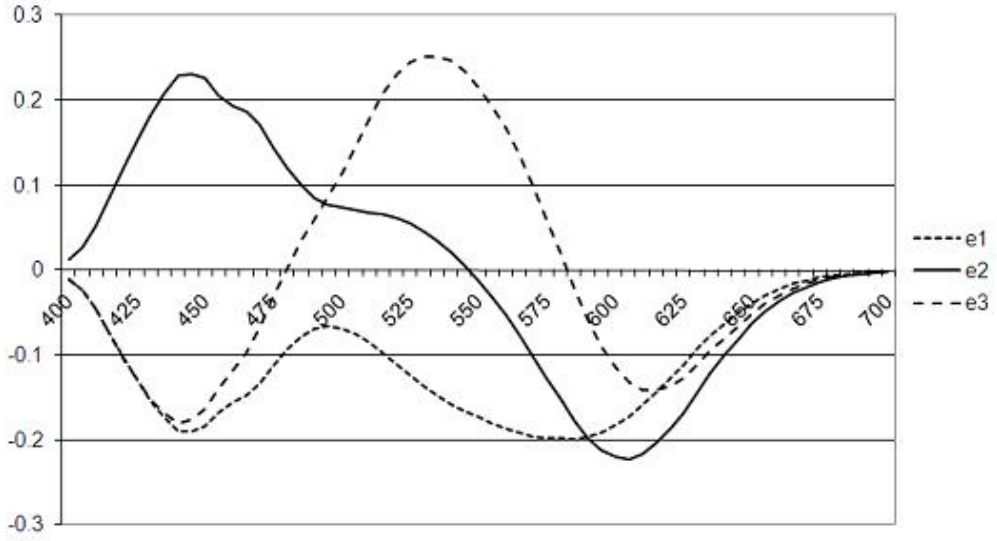

Figure 2: Model wavelength dimensions from the SVD of projected cube-rooted reflectance spectra.

The first dimension of the space closely fits Munsell Value; Romney & Chiao (p.10378) report that model output for Munsell chips on their first dimension correlates 0.9992 with L* coordinates in CIE L*a*b* (which is connected to Value). This is perhaps surprising, as the e1 curve differs from the luminous efficiency function used in determining L* values. Interestingly, Schrödinger (1920/1970, p.164) derived a similar brightness curve, but dismissed it as "completely impossible … a hideous camel's back." Despite its "hideous" nature, this Bactrian curve has the virtues of having its two humps crest within five nanometers of the two wavelengths known to jointly maximize luminosity in artificial lights, 450 and 580 nm, and having a local minimum at 495 nm, a wavelength that impairs luminous efficiency in lights (Thornton 1971, p.1157). Dimensions e2 and e3 are chromatic. Figure 3 depicts, based on the current analysis, the Munsell chips and spectral envelope collapsed on the chromaticity plane; this figure agrees with Romney & Chiao's figure 2.b (p.10379). About the spectral envelope points, the model predicts that a monochromatic stimulus of a given wavelength would share a

hue with the Munsell chips falling on the same radial line from the origin in the chromaticity plane. Figure 4 shows the locations in the chromaticity diagram of all plant reflectances generically labeled “red” or “green.” The only manipulations to the model’s output are a change of sign for raw x-axis values and a short rigid movement of each structure to place the achromatic chips at the origin.

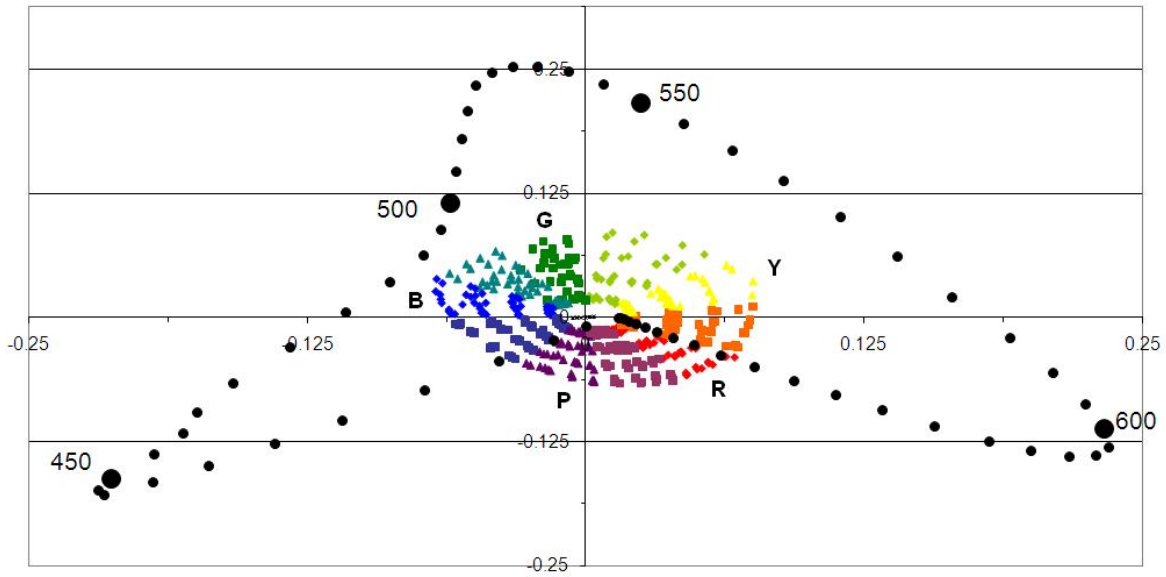

Figure 3: Locations of Munsell chips and the spectral envelope in the chromaticity plane of Romney & Chiao’s model. The five principal Munsell Hue sectors are indicated by corresponding letters. Some spectral envelope wavelength locations are labeled to aid interpretation. Pseudo-colors are used to represent Hue sectors.

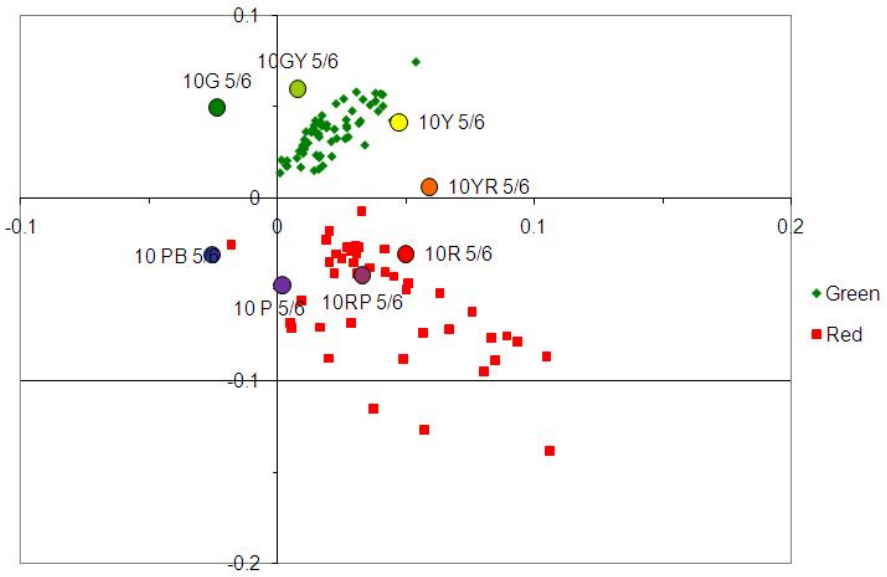

Figure 4: Locations of all plant samples with the generic labels "green" or "red." Locations for Munsell chips of Value 5, Chroma 6 of several Hues are included to aid interpretation. Pseudo-colors are used to represent generic hue designations.

Romney & Chiao's cube-rooting of reflectance spectra has affinities to nonlinear operations applied to tristimulus values in converting, for example, from CIE XYZ to CIE L*a*b*. However, their cube-rooting of reflectance spectra is justified on entirely pragmatic grounds (p.10377). It is not interpretable in terms of material properties of objects or the interaction of light and matter, and it is implausible to suppose that the retina could estimate and cube-root a surface's spectral reflectance prior to the stage of processing represented by the projection matrix. Cube-rooting reflectance spectra delivers a cylindrical color space in which stimuli of identical Hue and Chroma but different Value "stack" vertically, forming nested chroma cylinders throughout. Without this step, reflectance-based models produce a cone, with rings of constant Chroma that expand with increasing Value; see Burns et al (1990, pp.33,38-48, figs.5,12). As equal Chroma steps should be perceptually equivalent throughout color space, the cube-rooting is essential.

One might worry about a decidedly nonintuitive step playing a vital role in the model, however good its results. Romney & Chiao's cube-rooting of reflectance spectra could, though, be viewed as a shortcut for a more plausible process. Consider (1):

1. $(x^{1/3} * y) = (x * y^3)^{1/3}$

Cube-rooting reflectance spectra before they are run through the projection matrix allows the use of standard matrix multiplication to generate $\underline{S}$. However, (1) entails that the same $\underline{S}$ could be derived using raw reflectance spectra and a cubed (element-wise) projection matrix. The raw reflectance matrix would be multiplied by the cubed projection matrix in such a way that each product of the respective row and column entries is cube-rooted before summing them in the usual manner for matrix multiplication to determine the entries of $\underline{S}$.[8] This moves the cube-rooting within the visual system, where there are nonlinearities, without requiring an estimate of a spectral reflectance at the retina.

Returning to the model output, it might be surprising that almost all "green" plant samples fall in GY, rather than G. This is due to the optical properties of chlorophyll, the pigment primarily responsible for greenish appearance in plants; see Lee (2007, chpt.3). The reflectances of GY Munsell chips resemble those of biological samples routinely categorized as green. Figure 5 shows the reflectance spectra of Munsell chip 5GY 5/6 and a maple leaf with balanced chlorophyll and carotenoid content (based on #4 in figure 2 of Gitelson et al 2002), and a curve representing the mean of the 62 "green" plant spectra analyzed here. I turn now to some details of the spectral envelope.

---

[8] For example, the $\underline{i,j}$ entry of $\underline{S}$, given a raw reflectance matrix $\underline{A}$ of four columns and an element-wise cubed projection matrix $\underline{P^3}$ of four rows, would be: $\underline{(A_{i1} * P^3_{1j})^{1/3} + (A_{i2} * P^3_{2j})^{1/3} + (A_{i3} * P^3_{3j})^{1/3} + (A_{i4} * P^3_{4j})^{1/3}}$. Strictly speaking, since the projection matrix includes negative values, the cube-rooting involves solving for the $\underline{z}$ that satisfies $\underline{w = z^3}$.

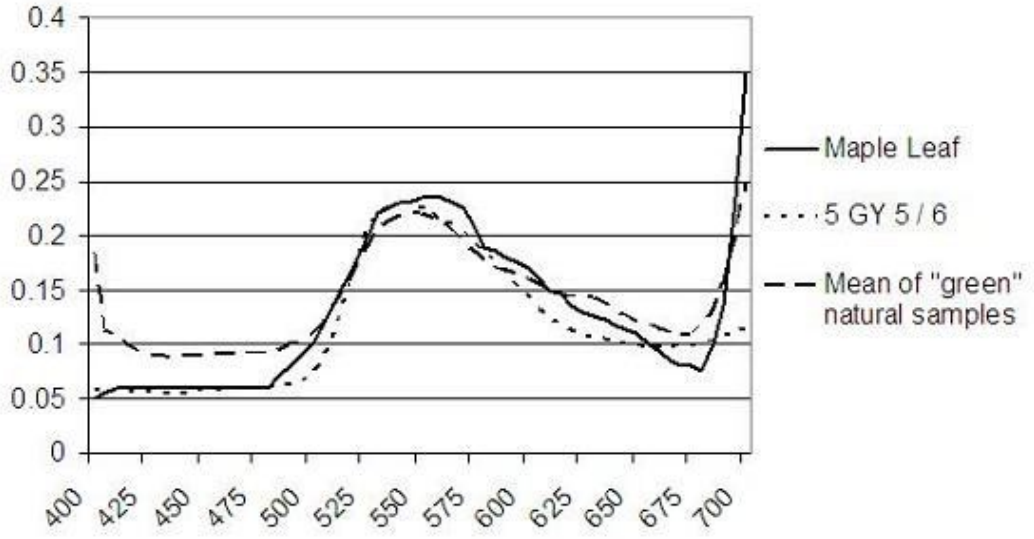

Figure 5: Reflectance spectra for a maple leaf and Munsell chip 5GY 5/6, and the mean reflectance spectrum for the 62 plant samples with the generic label "green."

3. Thornton's prime colors

William Thornton (1971; 1999) discovered a set of three primary lights that optimize between the color-rendering and luminosity performance of artificial illuminants. Those criteria conflict, as the illuminant characteristic most conducive to maximizing the range of perceivable colors is a flat power spectrum, while luminosity is maximized by limiting the illuminant spectrum to two narrowband spikes at 450 and 580 nm (Thornton 1971, pp.1157-1158). The prime colors discovered by Thornton occur near 450, 535, and 610 nm. Thornton also found anti-prime colors that are "disastrous" for use in artificial illuminants. They are around 490 and 570 nm. The precise reported prime and anti-prime wavelengths vary slightly across Thornton's publications; cf. Thornton (1971, p.1158) and Thornton (1999, pp.153-154). Godlove (1947), Hurvich & Jameson (1955), and MacAdam (1938), among others, had previously noted interesting properties of Thornton's prime and anti-prime locations.

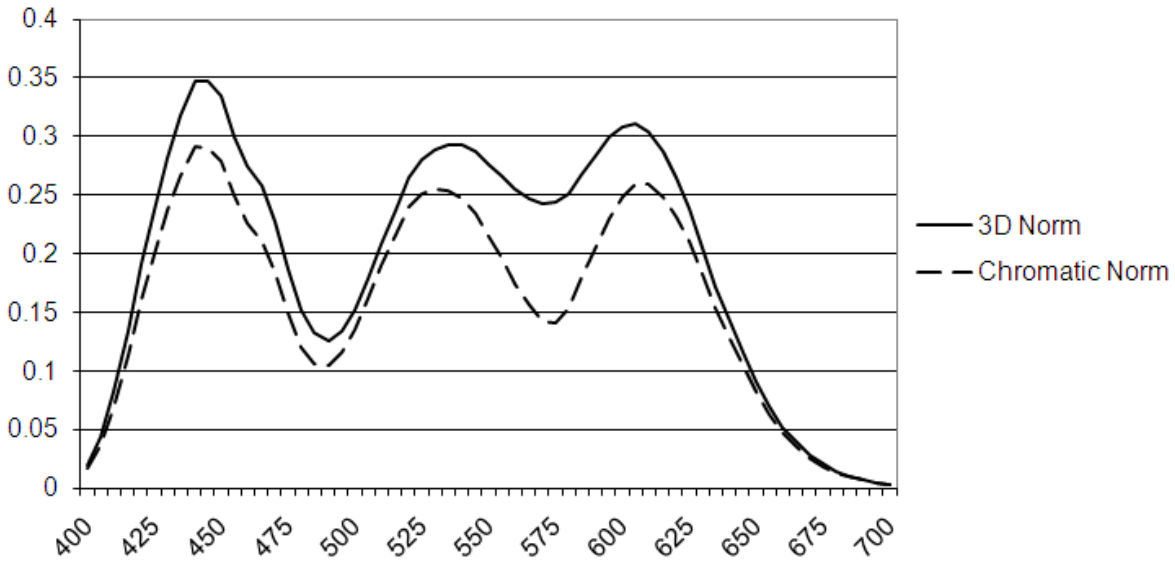

Figure 6: Norms for spectral envelope locations in both the three-dimensional space and the chromaticity plane of the Romney & Chiao model.

Figure 6 plots the Euclidean distances from the origin (norms) of the spectral envelope points in the current replication of the Romney & Chiao model, based on the curves in figure 2. The extrema in figure 6 tally with Thornton's primes and anti-primes. Suggestive for the coming discussion is that in Abramov & Gordon's hue scaling research (1994, p.459, fig.1a; 2005, p.2145, fig.1a), the wavelengths at which mean hue functions are balanced (e.g., 50% blue and 50% green) for blue-green, green-yellow, and yellow-red are (or are in the immediate vicinity of) 490, 570, and 610 nm, respectively.

4. Predictions from Jameson & D'Andrade's conjecture

The first step in assembling the pieces that have been set out is to generate predictions about locations around which unique hue judgments should bunch, based on Jameson & D'Andrade's (1997, p.314) conjecture that the Hering primaries coincide with points of distinctive ratios of chromatic to achromatic sensitivity. Using curves from figure 2 and 6, figure 7 shows the ratio of

chromatic response (norms of <e2, e3> points) to achromatic response (norms of <e1> points), as a function of wavelength. Ignoring very short and very long wavelengths, where there is little change in perceived color, the extrema of that curve (using a five-point stencil to approximate where the curve's first derivative goes to zero) occur at 475-480 nm, 510-515 nm, 575 nm. Based on figure 3, those locations on the spectral envelope approximately correspond to Munsell Hues 2.5PB, 7.5G, and 5Y.

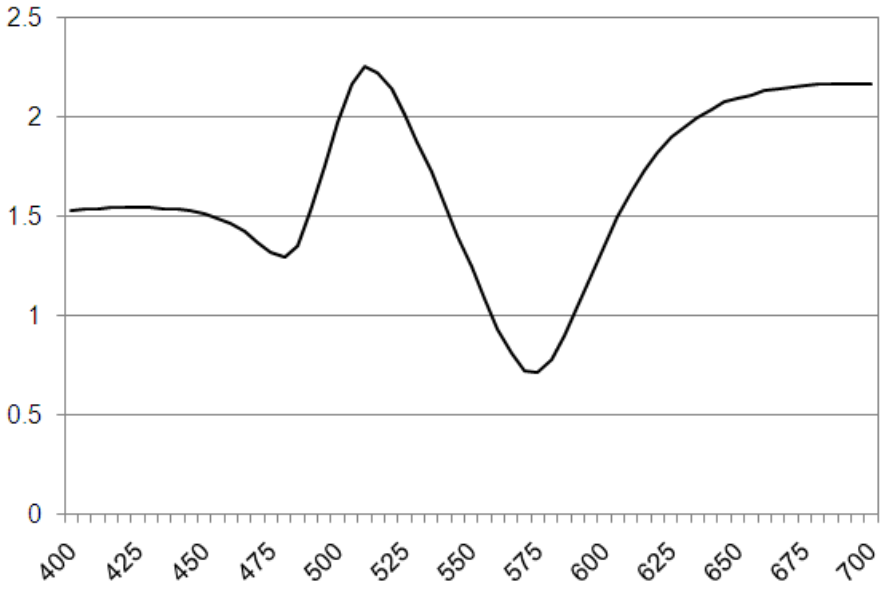

Figure 7: Ratio of chromatic to achromatic response, based on curves in figures 2 and 6.

The locations just noted align well with hue scaling and unique hue findings for both lights and Munsell chips; the studies cited here are representative of the literature, as can be seen through a comparison with the review of experimental data in Kuehni (2004). The mean hue functions for blue, green, and yellow reported by Abramov & Gordon (2005, p.2145, fig.1a; 1994, p.459, fig.1a) for hue scaling with spectral lights peak at 470, 520, and 580 nm, respectively. They also report mean unique hue judgments for blue, green, and yellow at ~468,

~512, and ~578 nm (Abramov & Gordon 2005, p.2145, fig.1d). For unique hue judgments with broadband lights, the mean dominant wavelengths for blue, green, and yellow in Webster et al (2000, pp.1549-1550, tables 1 and 2) are 477, 545, and 574 nm; this discrepant unique green point will be returned to. As for unique hue choices with Munsell chips, Hinks et al (2007, p.3375, fig.4) show blue, green, and yellow means of 9B, 10G, and 3.75Y. Kuehni (2001, p.63, table I) finds mean unique blue, green, and yellow at 2.75PB, 2.5BG, and 3.5Y and elsewhere mentions a dataset with a mean unique green of 7G (Kuehni 2003, p.140).

While the concordances just noted suggest that Jameson & D'Andrade's conjecture is on the right track, two further matters warrant attention. First, unique red has not been addressed. Unique red is extra-spectral and thus wavelength data are not available for it. It is as yet unclear how a prediction for unique red Munsell selections might be generated from chromatic/achromatic response ratios. Second, all that has been done so far is to observe that certain points around which unique hue judgments collect fall at or nearby distinctive features of spectral sensitivity. Some details about the emergence of hue categories around those points would be helpful. The next section deals with these issues, focusing on the prime and anti-prime colors.

5. Hue categories and the prime/anti-prime colors

Figure 8 shows the first derivatives of the three-dimensional norm curve from figure 6, based on a five point stencil approximation. As they indicate local maxima or minima of overall response, the zero-crossings from figure 8 will be used for prime and anti-prime colors: 445, 535, and 605 nm for the primes (switch from positive to negative) and 490 and 570 nm for the anti-primes (switch from negative to positive). Those critical points also mark where the rate of change of

response due to small variations in wavelength should be lowest.[9] Such regions are likely candidates for borders between hue categories, as we do not experience an abrupt break between, say, blue and green, but rather a gradual transition between them. In tandem with this, one might also suppose that the focal exemplars of hue categories should tend to fall at local peaks in sensitivity to wavelength changes, the intuition being that sensitivity to differences seems much finer around the unique Hering primaries. The maxima between zero-crossings in figure 8 are 475, 510, 555, and 585 nm. Two of those match members of the set generated based on Jameson & D'Andrade's conjecture (475 and 510 nm), one is not present at all in that set (555 nm), and another falls 10 nm beyond its counterpart in that set (585 nm). This method of predicting where unique hue selections should cluster turns out to not fare as well as the one canvassed in the preceding section, but it raises some interesting issues that make it worth including.

[9] The focus on the rate of change of the sensitivity function is due to a helpful suggestion by Justin Broackes.

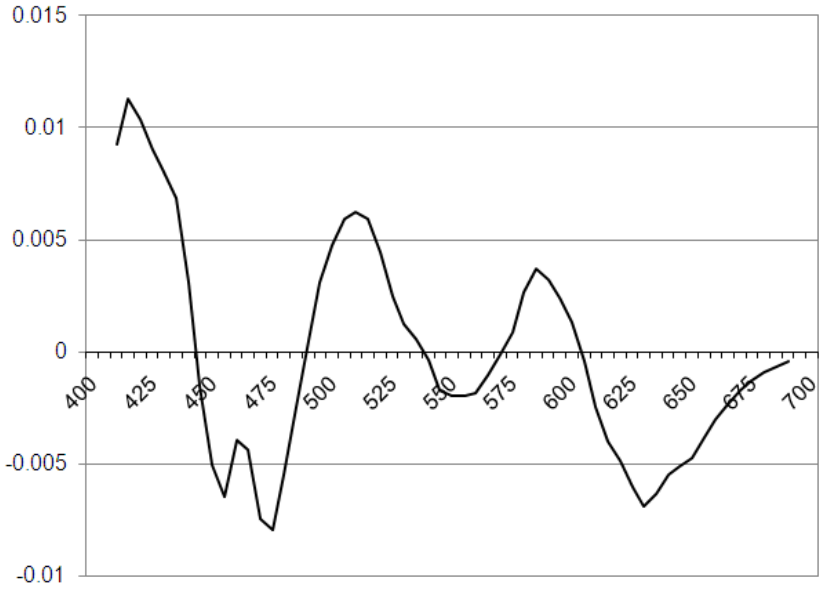

Figure 8: First derivatives of the curve of three-dimensional norms of spectral envelope points from figure 6.

Figure 9 replicates figure 3, but with prime and anti-prime locations marked and radial solid lines drawn to them from the achromatic origin. The line extending from the origin opposite the 535 nm prime is dashed to indicate that the point it terminates at is not one of Thornton's prime or anti-prime colors, but is related to them in being a local extremum of overall response. This point has the smallest three-dimensional norm of points on a line between 445 and 605 nm (akin to the "line of purples" in CIE diagrams) and is the only zero-crossing of the first derivative curve for those three-dimensional norms. This local minimum of response seems just as legitimate a candidate for signaling a hue category boundary as the anti-prime wavelengths identified by Thornton. To avoid laborious expressions (e.g., "the two anti-primes and the extra-spectral point opposite the 535 nm prime"), I will refer to this extra-spectral location as an anti-prime. None of this is meant to imply that the extra-spectral point in question figures in Thornton's research.

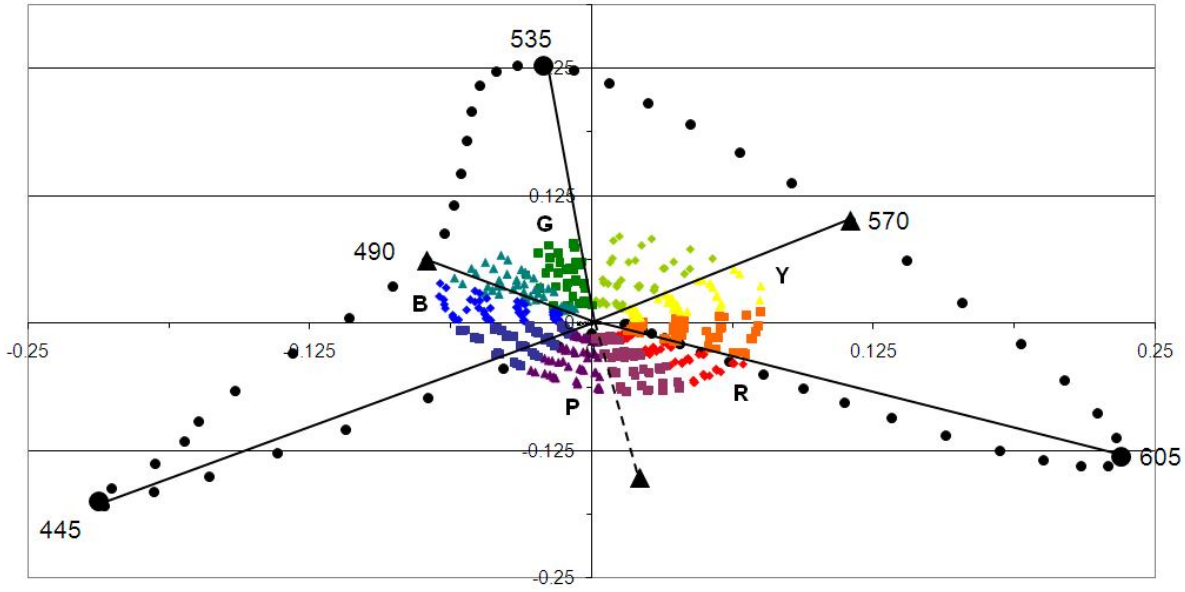

Figure 9: The same as figure 3, but with locations for the 445, 535, and 605 nm prime colors and 490 and 570 nm anti-prime colors labeled and connected to the achromatic origin with solid lines. The extra-spectral "anti-prime" is indicated with a dashed line.

The primes and anti-primes alternate in sequences around the hue circle. Something to notice about figure 9 is that there are basically two full hue sectors between each prime/anti-prime neighboring pair (e.g., PB and B between 445 and 490 nm), except that the Green-Yellow (GY) and Purple (P) regions are single hue sectors each bound by a prime and an anti-prime. The hypothesis to be explored is that the emergence of the Hering primaries is already well underway at the retina, based on how the prime and anti-prime colors delineate regions of color space.

About the two sectors between 445 and 490 nm, B and PB are qualitatively quite similar in a way that suggests linking this region to the hue category of blue; on the current results, the relevant range is about 7.5PB to 9BG. For one thing, the ranges of Munsell chips and wavelengths selected as unique blue are contained in this region. Kuehni (2005, p.400, fig.5)

reports the range of Munsell chips selected as unique blue (UB) by subjects across different studies as 7.5PB to 2.5B; Hinks et al (ibid.) show essentially the same range. For light stimuli, Webster et al (2000, pp.1549-1550, tables 1 and 2) found the range of dominant wavelengths for unique blue judgments with broadband stimuli to be 465-486 nm, while Abramov & Gordon's (2005, p.2150, fig.5a) subjects showed a range of 430-480 nm with monochromatic lights; aside from two of their fifty subjects, the latter range is 450-480 nm. Using the mean hue functions of Abramov & Gordon (1994; 2005), stimuli are judged to be less than 50% blue beyond 490 nm. On the short wavelength side, however, the mean percentage of perceived bluishness is still ca. 70% at 430 nm; presumably, the other 50% point for blue is an extra-spectral purple. So, in associating the region of the chromatic plane between 445 and 490 nm with blue, it is not implied that bluishness is absent in samples outside that range; e.g., 5B and 5BG are surely similar in some bluish respect despite falling in different prime/anti-prime regions. The idea instead is that the most characteristically blue stimuli fall within that region.

It has already been noted in discussing Jameson & D'Andrade's conjecture that the empirical data agree with the current prediction that mean unique blue choices from differing experiments should cluster around 475 nm and its corresponding Munsell Hue of 2.5PB. Also relevant is that in a contour plot of World Color Survey (WCS) participants' "best exemplar" (focal color) choices for basic color terms of their language, one cluster peaks at 2.5PB (MacLaury 1997, p.202, fig.1).[10]

For the moment I will skip over the 490-535 nm and 535-570 nm regions and consider the Y and YR sectors that are fenced in by 570 and 605 nm. As with 445-490 nm and blue, there

[10] A language's basic color terms form the smallest set of simple terms that could be used to name any color. For more on basic color terms and focal choices, see Kay & Regier (2003).

is good reason to think that stimuli which fall in this region are qualitatively similar in a way that justifies associating this region with the hue category of yellow. For one thing, Abramov & Gordon's (ibid.) mean hue scaling functions show judgments of balanced contributions between yellow and green at 570 nm and between yellow and red at 600-610 nm. This region includes the entire range of Munsell chips selected as unique yellow, as Kuehni (ibid.) reports a range of 10Y to 7.5YR; Hinks et al (ibid.) display a comparable range. Webster et al (ibid.) found a dominant wavelength range of 570-580 nm for unique yellow settings with broadband lights, while Abramov & Gordon's (ibid.) subjects' choices for unique yellow ranged from 570 to 590 nm with spectral lights. Also, most languages from the WCS use one term to designate both yellow and orange (Kay & Regier 2003, p.9089).

The mean choices for unique yellow stimuli, with both Munsell chips and light stimuli, fall on the short wavelength side of the current prediction of 585 nm, which corresponds to ~7.5YR; recapping the mean data, with lights unique yellow falls in the neighborhood of 575 nm and with Munsell chips it is near 3.5Y. Also relevant is that WCS focal color choices have a peak at 2.5Y (MacLaury ibid.). As noted before, the prediction for unique yellow generated from Jameson & D'Andrade's conjecture holds up well. This discrepancy is interesting in the light of the fact that some researchers have hypothesized that there is a cortical mechanism that "tunes" perceivers' unique yellow points to roughly the same location around 575 nm, without affecting their other unique hue points; see Abramov & Gordon (2005, p.2151). The reason for supposing there is such a mechanism is that there is very little variation in unique yellow settings across different subjects. Such small variation is notable, considering the polymorphisms in L and M cone sensitivities and that unique hue ranges for the other Hering primaries are much wider.

The R and RP sectors are bound by the 605 nm prime and the extra-spectral "anti-prime." Again, this is a region of high qualitative similarity that naturally connects it with a hue category; in this case, red. For Munsell chips selected as unique red, Kuehni (2001) reports a range from 9R to 6RP, while Hinks et al (ibid.) show a range of 10R to 3.75RP. Note too that the vast bulk of "red" natural reflectances fall in the R and RP sectors in figure 4. Although wavelength data are not available for unique red ranges, it is relevant that in Abramov & Gordon's hue scaling studies the point of balanced hue judgments between yellow and red occurs right around 605 nm.

Regarding mean unique red judgments, a prediction cannot be generated from the first derivative curve for the three-dimensional norms of points on the line connecting 445 and 605 nm, as it is monotonic. Additionally, applying Jameson & D'Andrade's conjecture to points on that line produces a U-shaped curve that bottoms out at a point in P near its border with RP. Not only is that point unhelpful when it comes to unique red, it is not a good prediction for focal purple (5P). Thus identifying a focal exemplar for red is beyond the reaches of the resources presented herein. However, it is worth pointing out that subjects' mean unique red judgments with Munsell chips fall in the middle of the R/RP region established by the 605 nm prime and extra-spectral "anti-prime." Hinks et al (ibid.) have a mean unique red at 2.5R and Kuehni (2001) relates a mean unique red at 3R. In the WCS data, the focal exemplar plot has a peak at 2.5R (MacLaury ibid.).

While the current method for determining hue category borders shows good agreement with empirical results, and the method based on Jameson & D'Andrade's conjecture has done well with unique blue and unique yellow, matters with green are complicated. Unique green is notorious for the wide variability of stimuli selected as evincing it. The range of Munsell chips selected as unique green covers the BG and G sectors bound by 490 and 535 nm, as well as a

slight (and quite rare) intrusion into B (2.5B) and a more significant (and much more common) foray out to 5GY (Kuehni ibid.). The range of dominant wavelengths for nonspectral lights judged as unique green runs 490-560 nm (Webster et al ibid.), with a similar span (490-550 nm) for monochromatic lights (Abramov & Gordon ibid.). As mentioned previously, several mean unique green results agree with the predictions of 510 nm and 7.5G made by both methods considered here, but the location found by Webster et al (2000) is considerably off from it; the findings summarized in Kuehni (2004, p.160) show this sort of bimodality for unique green. Also, in the WCS data, a cluster of focal exemplar choices peaks at 2.5G, which is in line with the 535 nm prime. Abramov & Gordon's balanced hue judgment results for green are noteworthy, as well. The balance point between blue and green falls at the 490 nm anti-prime and the balance point between green and yellow occurs at the 570 nm anti-prime. At the 535 nm prime, the mean hue function for green has a value only slightly less than that at the ~515 nm mean unique green point. Lastly, the 555 nm peak in figure 8 is at the far long wavelength end of the range of stimuli selected as unique green and is never selected as unique yellow.

So, while it might be tempting to straightforwardly tie green to 490-535 nm, in similar fashion to how the other Hering primary categories correspond to prime/anti-prime regions, much of the available data is clearly inconsistent with such a move. This situation appears to connect with the isolation of the GY sector in the model. Perhaps also relevant is that the 555 nm peak in figure 8 does not show up as a local extremum in the curve in figure 7 representing the ratio of chromatic to achromatic sensitivity.

First, about GY, I propose that a reason for there being only one hue sector between 535 and 570 nm is the aforementioned clustering of "green" plant surfaces in the GY region. Suppose that the evolution of our color vision was strongly influenced by the demands facing our

antecedents in foraging for ripe fruit or proteinaceous young leaves amongst foliage. These are the "frugivory" and "folivory" hypotheses; see Osorio & Vorobyev (2007) and Dominy & Lucas (2004). In that circumstance, it would be beneficial to perceptually segregate mature leaves and stems so that they can easily be ignored while ripe fruits or young leaves are made to stand out markedly. Minimizing hue differences between bits of foliage while creating salient hue differences between nutritious objects and foliage would help achieve that. Many ripe fruits appear yellow, orange, or red, due to the carotenoids or flavonoids they contain; those pigments strongly absorb light in the short and middle wavelengths of the visible spectrum. Young leaves have a substantial flavonoid content and hence a reddish appearance. Thus the ripe fruits and young leaves are conspicuous amongst greenish-appearing, chlorophyll-rich mature leaves and stems; see Lee (2007, chpt.8) for more on plant pigments.

The demands of these biologically crucial tasks would account for the expansion in distance between hue radii in the 535-570 nm region of the spectral locus; short distances between points in this region of color space (corresponding to small variation in stimulus properties) are not associated with conspicuous hue differences. It would also stand to reason that there is not a local extremum of the chromatic/achromatic response ratio in this zone, if such extrema are indeed markers of perceptually distinctive regions of color space. Furthermore, it would make sense that GY is the only region carved out by a prime/anti-prime pair that does not map onto a psychologically basic hue, if it is advantageous for natural GY spectra to be easily ignored in biologically important tasks. Indow (1987) found that the Hering primaries and purple (the other isolated hue sector) are psychologically basic.[11]

[11] Psychologically basic hues are fundamental to the perceptual organization of the hues. The Hering primaries are obvious candidates for being psychologically basic. It turns out that purple,

The characteristics of GY just noted provide a plausible rationale for the tendency of some results to be pulled away from the predicted location of 510 nm and toward the GY sector. Kuehni (2004, p.162) suggests that "the pervasive nature of green in the natural environment of many people, and certainly for our early ancestors, may offer an explanation for the large variability in [unique green]." Prolonged or focal exposure to such often ubiquitous and important stimuli, under viewing conditions that can vary across time and place, may cognitively influence subjects' judgments about unique green (e.g., affecting their criteria for what an ideal green should look like) or change their visual system's post-receptoral state of adaptation and thus alter the relationship between their personal color space and stimulus properties; see Webster et al (2002, p.1960) and McDermott et al (2008).

Chartreuse (GY) is not presented to us as a distinctive hue region admitting of fine discrimination of subtle stimulus differences at its center; this is reflected in the fact that the 555 nm peak in figure 8 is dwarfed by the other extrema between zero-crossings. Additionally, distinctive differences between chromatic and achromatic responses are not found in that sector. Thus it is understandable that chartreuse would not emerge as a hue category on a par with the Hering primaries. Subjects find it natural to classify GY stimuli as predominantly greenish, along with stimuli that plot in the 490-535 nm range. There is clearly a sense in which, for example, 5G and 5GY are similar in a greenish respect, just as 5B and 5BG have a similarity in terms of bluishness. On the other hand, while 2.5Y and 2.5GY stimuli are similar in some yellowish

---

while being composed of reddishness and bluishness, also has a claim to being psychologically basic. Purple helps "sharpen concepts of pure red and pure blue" (Indow 1987, p.255), as including it (rather than using the four Hering primaries alone) as a principal hue markedly reduces individual differences in ratings of the degrees of red and blue perceived in stimuli; see figures 2 and 3.I in Indow (1987, p.256).

respect, it is clear from the unique hue, hue scaling, and WCS data noted above that there is not a tendency for perceivers to judge GY stimuli as being highly representative of yellow. The importance of seeing yellowish ripe fruits as distinct from their surrounding foliage would explain why GY stimuli (like mature leaves) appear as predominantly greenish, rather than yellowish.

So, although low-level sensitivity makes a division in color space that isolates the GY sector in a manner with biologically useful effects on hue perception, that isolation does not carry over to the perceptual organization of the hues as a distinctive, basic hue category. At some point in the neural processes leading to color experience, the 490-535 nm and 535-570 nm prime/anti-prime regions are conjoined as a single hue category, green. Again, the claim is not that greenishness is confined to 490-570 nm, but rather that the most characteristically green stimuli fall in that span; recall the balanced mean hue functions at 490 and 570 nm. Given that several studies find a mean unique green near the 510 nm location predicted by both methods considered here, for some observers the details of spectral sensitivity at the retina would seem to strongly influence what stimuli are judged most purely green. For other perceivers, though, greater weight is given to some other factor(s), drawing unique green judgments in the direction of GY. This plasticity in the weighting of factors that contribute to unique green judgments stands in stark contrast to the hypothesized cortical preference for a specific unique yellow point.

As for the P sector (plus 10PB) bound by the 445 nm prime and the extra-spectral "anti-prime," Indow's (1987) research on psychologically basic hues suggests that there is something perceptually distinctive about that region. One might take this distinctiveness to support Jameson & D'Andrade's (1997) challenge to the received Hering opponent colors theory, particularly their questioning of the rationale for preferring the entrenched four-basic-hues model to a five-

basic-hues model (p.311). Conversely, one might retain the standard four-basic-hues-model, point to the phenomenological forcefulness of the idea that purples are perceptually composed of reddishness and bluishness, and claim that low-level features of spectral sensitivity give such composite hues certain properties that distinguish them from other binary combinations of Hering primaries. Those additional properties would be such that they do not justify treating purple as being on a par with the Hering primaries, at least in certain crucial respects. Addressing these options, as well as any others that might be introduced, is beyond the scope of this paper. What matters for present purposes is that however the "specialness" of purple is to be understood, a basis for singling it out in some way is already manifest at the retina.

6. Conclusion

The way of thinking about the hues offered here has it that features of low-level spectral sensitivity are fundamental to the emergence of perceptual hue categories and unique hue percepts. Specifically, maxima and minima of sensitivity to small wavelength changes provide for the development of hue category boundaries, while the ratio of chromatic to achromatic sensitivity is relevant to the determination of focal examples of those categories. About the latter, Jameson & D'Andrade's conjecture about the ratio of chromatic to achromatic sensitivity clearly outperforms the predictions based on the three-dimensional norms of spectral envelope points. Besides inter-observer variability in hue scaling and unique hue tasks, other issues are not resolved by this account, at least not fully: the location of unique red, at what point and how the isolated GY sector is perceptually grouped together with the paired-off BG and G sectors as highly representative of green, and in what the specialness of purple consists. Nonetheless, this

account does promise to help improve our knowledge of hue phenomena, as it makes clear how much of the nature of the hues is already present at the outer reaches of the visual system.

7. References

Abramov, L. & J. Gordon. 1994. "Color appearance: on seeing red – or yellow, or green, or blue." Annual Review of Psychology, 45,451-485.

_____. 2005. "Seeing unique hues." Journal of the Optical Society of the Optical Society of America A, 22, 2143-2153.

Buchsbaum, G. & A. Gottschalk. 1983. "Trichromacy, opponent colours coding and optimum color information transmission in the retina." Proceedings of the Royal Society of London (B), 220, 89–113.

Burns S., J. Cohen, & E. Kuznetsov. 1990. "The Munsell color system in fundamental color space." Color Research and Application, 15, 29–51.

Changizi, M., Q. Zhang, & S. Shimojo. 2006. "Bare skin, blood and the evolution of primate colour vision." Biology Letters, 2, 217-221.

Cohen, Jonathan & M. Matthen (eds.). 2010. Color Ontology and Color Science. Cambridge (MA): MIT Press.

Cohen, Jozef. 2001. Visual Color and Color Mixture. Chicago: University of Illinois.

De Valois, R. & G. Jacobs. 1968. "Primate color vision." Science, 162, 533-540.

Dominy, N. & P. Lucas. 2004. "Significance of Color, Calories, and Climate to the Visual Ecology of Catarrhines." American Journal of Primatology, 62, 189-207.

Gitelson, A. Y. Zur, O. Chivkunova, & M. Merzlyak. 2002. "Assessing carotenoid content in plant leaves with reflectance spectroscopy." Photochemistry and Photobiology, 75, 272-281.

Godlove, I.H. 1947. "The limiting colors due to ideal absorption and transmission bands." Journal of the Optical Society of America, 37, 778-791.

Hardin, C.L. & L. Maffi (eds.). 1997. Color Categories in Thought and Language. Cambridge: Cambridge University Press.

Hinks, D., L. Cardenas, R. Kuehni, & R. Shamey. 2007. "Unique-hue stimulus selection using Munsell color chips." Journal of the Optical Society of America (A), 24, 3371-3378.

Hurvich, L. & D. Jameson. 1955. “Some Quantitative Aspects of an Opponent-Colors Theory. II. Brightness, Saturation, and Hue in Normal and Dichromatic Vision.” Journal of the Optical Society of America, 45, 602-616.

Indow, Y. 1987. “Psychologically unique hues in aperture and surface colors.” Die Farbe, 34, 253-260.

Jameson, K. & R. D’Andrade. 1997. “It’s not really red, green, yellow, blue: an inquiry into perceptual color space.” In Hardin & Maffi (1997).

Kay, P. & T. Regier. 2003. “Resolving the question of color naming universals.” Proceedings of the National Academy of Sciences, 100, 9085-9089.

Koenderink, J. & A. van Doorn. 2003. “Perspectives on colour space.” In R. Mausfeld & D. Heyer (eds.). Colour Perception: Mind and the Physical World. London: Oxford University Press.

Kohonen, O., J. Parkkinen, & T. Jaaskelainen. 2006. “Databases for spectral color science.” Color Research and Application, 31, 381-388.

Kuehni, R. 2001. “Determination of unique hues using Munsell color chips.” Color Research and Application, 26, 61-66.

_____. 2003. Color Space and Its Divisions. Hoboken (NJ): John Wiley & Sons.

_____. 2004. “Variability in unique hue selection: A surprising phenomenon.” Color Research and Application, 29, 158-162.

_____. 2005. “Unique hue stimulus choice: a constraint on hue category formation.” Journal of Culture and Cognition, 5, 387-407.

Lee, D. 2007. Nature’s Palette: The Science of Plant Color. Chicago: University of Chicago Press.

MacAdam, D. 1938. “Photometric Relationships Between Complementary Colors.” Journal of the Optical Society of America, 28, 103-111.

_____. 1953. “Dependence of color-mixture functions on choice of primaries.” Journal of the Optical Society of America, 44, 713-724.

_____ (ed.). 1970. Sources of Color Science. Cambridge, MA: MIT Press

MacLaury, R. 1997. “Ethnographic evidence of unique hues and elemental colors.” Behavioral and Brain Sciences, 20, 202-203.

MacLeod, D. 2010. “Into the neural maze.” In Cohen & Matthen (2010).

McDermott, K., I. Juricevic, G. Bebis, and M. Webster. 2008. “Adapting images to observers.” In B. Rogowitz & T. Pappas (eds.), Human Vision and Electronic Imaging, SPIE Proceedings, 68060V-1-10.

Osorio, D. & M. Vorobyev. 2007. “Colour Vision as an Adaptation to Frugivory in Primates.” Proceedings: Biological Sciences, 263, 593-599.

Romney, A.K. & C.C. Chiao. 2009. “Functional computational model for optimal color coding.” Proceedings of the National Academy of Sciences, 106, 10376-10381.

Schrödinger, E. 1920/1970. “Outline of a theory of color measurement for daylight vision.” In MacAdam (1970).

Stockman, A. & L. Sharpe. 2000. “The spectral sensitivities of the middle- and long-wavelength- sensitive cones derived from measurements in observers of known genotype.” Vision Research, 40, 1711–1737.

Thornton, W. 1971. “Luminosity and color-rendering capability of white light.” Journal of the Optical Society of America, 61, 1155-1163.

_____. 1999. “Spectral Sensitivities of the Normal Human Visual System, Color-Matching Functions and Their Principles, and How and Why the Two Sets Should Coincide.” Color Research and Application, 24, 139-156.

Webster, M., E. Miyahara, G. Malkoc, & V. Baker. 2000. “Variations in normal color vision. II. Unique hues.” Journal of the Optical Society of America A, 17, 1545-1555.

Webster, M., S. Webster, S. Bharadwadj, R. Verma, J. Jaikumar, J. Madan, & E. Vaithilingam. 2002. “Variations in normal color vision: III. Unique hues in Indian and U.S. observers.” Journal of the Optical Society of America A, 19, 1951-1962.